

# Numerical Simulation On Packing Density Of Spherical Particles With Normal Distribution

Huadong Yang, Shiguang Li

Department of Mechanical Engineering, North China Electric  
Power University, Baoding, China, 071003

## ABSTRACT

Numerical simulation about the packing density of spherical particles with normal distribution of particle size was carried out by discrete element method (DEM) software. First, the model of mono-sized spherical particles (30 $\mu$ m) was established to verify the rationality of numerical simulation. Second, it was found that for spherical particles with normally distributed particle size, the packing density is generally higher than mono-sized particles (theoretical packing density is 0.7406). By analyzing the porosity change curve of spherical particles with different variance( $\sigma$ ), the results show that with the increase of  $\sigma$ , the porosity decreases firstly and then increases, which is opposite to the trend of packing density. By comparing the simulation results with Horsfield compact packing theory, it was demonstrated that the packing density of spherical particles with normally distributed particle size is generally between 0.7406 (unitary spherical particles) and 0.793 (binary spherical particles). And also, when the spherical particle model parameter is  $\mu=30\mu$ m and  $\sigma=20$ , the packing density reaches a maximum value 0.795, which is slightly higher than the theoretical packing density of the binary spherical particles.

Date Of Submission:05-10-2018

Date Of Acceptance: 17-10-2018

## I. INTRODUCTION

In the particle research field, particle packing has always been a very important research issue [1-7]. Scientists devote to find the method to increase the packing density of particles, and also study the physical characteristics of the accumulation of different particles. In the late 1920s, Smith et al. [8] began to study the accumulation of spherical particles. Nowadays, many researchers focus on the discussion of particle packing density.

As early as 400 years ago, scientist Kepler predicted that the maximum packing density of hard spheres with the same size will not exceed 0.74, that

is the packing density of face centered cubic (FCC) or hexagonal close packing (HCP) structure. This conclusion has been proved mathematically[9]. The pioneer in physical experiments was Bernal et al. [10]. The results of the study showed that the random accumulation of identical spheres can provide a useful model for the study of ideally simple fluids. Scott [11] found that the maximum random packing density of 20,000 steel balls with a diameter of 3.175mm can reach 0.63 in a rigid container. Then scientific research workers conducted extensive research on the density of multi-particulate matter, mainly focusing on improving the overall particle

density through vibration measures, but on the study of the density of multi-particulate matter, especially the density of particles with a continuously distributed particle size, little research is involved. In general, the particle size distribution of particles is in a nearly normal distribution, especially in areas where there are special requirements for particulate matter. For example, metal 3D printing technology that has been booming in recent years is used to form metal particles, usually spherical or near-spherical metal particles with a roughly normal particle size distribution.

## II. PACKING MODELS AND THEORY

Many researchers study the particle packing density by theoretical calculations, numerical simulations and physical experiments. Owe Berg et al. [12] put 3.175mm diameter steel balls of 5000 numbers into a 63mm diameter cylindrical vessel, and then supplemented with 3D vibrations. It was found that the resulting arrangement was an orderly HCP structure. The corresponding packing density is close to 0.74. An Xizhong et al. conducted a series of experimental studies on the dense packing of primary and binary spherical particles under vibration conditions [13-15], and founded that the maximum packing density was 0.88. Scientific researchers have built a solid foundation for the in-depth research and development of particulate matter accumulation.

Segregation Packing Theory, also known as Zhang Rongzeng Theory, presupposes that the ratio of the natural accumulation particle size  $D$  and its pore size  $P$  is equal to the sieve ratio  $B$ . So the material is divided into several grades according to the sieve ratio  $B$ . Assume that in a continuously distributed material, if the volume of all particles in the  $i+1$  level is smaller than the volume of the  $i$  level gap, and the volume of the particles in the  $i+2$  level is exactly equal to the volume of the  $i$  level gap, then the closest packing can be achieved.

$$n = \ln \left( \frac{1}{\epsilon} \right) / \ln B \quad (1)$$

Where  $n$  is the modulus of the Gaudin and Alfred

equations,  $P$  is the porosity of the particles, and  $B$  is the sieve ratio. Through computer simulations, when the modulus  $n$  of the above equation is 0.37, the material has the closest packing.

(2)

In the formula,  $U$  represents the particles less than the particle size  $D$ ,  $D_{max}$  represents the maximum particle size,  $D_{min}$  represents the minimum particle size, and  $n$  represents the modulus.

In the natural world, normal distribution is widespread. For the metal 3D printing, metal powder particles can be prepared by reduction, atomization, electrolysis, mechanical pulverization, hydroxylation, direct chemical method and other methods [16-20]. Among them, the powders produced by the reduction method, the electrolysis method, and the atomization method are commonly applied to the powder metallurgy industry as raw materials. The resulting powder particles are micron-sized, high sphericity and normal particle size distribution.

As for the particle size distribution, a certain measurement method is often required. The particle size distribution and mass distribution are commonly used to define the degree of particle dispersion. The degree of dispersion is the ratio of the number (mass or surface area) of particles in different particle sizes in a certain particle body.

The particle size distribution function is commonly including normal distribution function, lognormal distribution function, and Rosin-Rammler distribution function. Because the amount of particulate matter is generally very large, the particle size distribution of the particle group is approximately a smooth curve, and the particle size deviation phenomenon is not obvious. Secondly, in the actual sedimentation process of the particulate matter, the smaller particles are likely to be suspended or collided. So, there is a tendency for large particles to sink quickly, further balancing the internal particle distribution of the particles after settling. Therefore, this paper mainly about the packing density of particles with a normally

distributed particle size.

The normal distribution function of the particles is:

$$P(d_p) = \frac{1}{\sigma\sqrt{2\pi}} \times \exp\left[-\frac{(d_p - \bar{d}_p)^2}{2\sigma^2}\right] \quad (3)$$

In the formula,  $\sigma$  and  $\bar{d}_p$  are two eigenvalues of normal distribution,  $\bar{d}_p$  is the average particle diameter,  $\sigma$  is the standard deviation, and its value determines the dispersion of particle size.

(4)

In the formula,  $d_{p_i}$  represents the representative particle of the  $i$  particle size segment,  $n_i$  represents the number of particles in the  $i$  particle segment, and  $N$  represents the total number of particles.

### III. NUMERICAL SIMULATION

In the field of metal 3D printing, it is required that the metal powders have characteristics such as fine grain size, narrow particle size distribution, high sphericity, good fluidity, and high packing density. Generally, two kinds of powders are used for metal 3D printing. One is fine powder with a particle size ranging from 15 to 53 $\mu$ m, and the other is a coarse powder with a particle size range of 53 to 105 $\mu$ m. Sometimes they are mixed together for meeting the requirements of metal 3D printing.

This paper selects fine powder as the main particle size distribution model and reduces the overall model size by a factor of ten, to reduce the excessively high computer performance requirements in the simulation process. The particle size distribution is controlled by controlling the geometric standard deviation of the normal distribution function. At the same time, assuming all particles are spheres, the friction coefficient and damping coefficient between the spheres and between the sphere and the wall remain the same by using the EDM (Discrete Element Method). The particle program command

software is chosen to simulate the generation of particles, natural sedimentation process and calculation of the final particle packing density. Thus, the best particle distribution function can be obtained in order to improve the performance of metal 3D printing.

#### 3.1 Set initial conditions

This paper simulates a spherical particle model with a mean particle size of  $\mu=30\mu$ m. The assumptions are as follows:

- (1) Apply a cylindrical boundary container, the ratio of the inner diameter of the container to the diameter of the sphere should be more than 20 to eliminate the effect of the boundary size as much as possible.
- (2) Set the measuring ball inside the measuring container to maintain a certain distance between the measured ball and the wall of the container, to eliminate the influence of the surrounding wall on the packing density of the particles inside the container.
- (3) The method of integral feeding is adopted, and the connection model between the spheres and the connection model between the sphere and the wall are set as a linear elastic model.
- (4) The values of the normal stiffness and tangential stiffness between spherical particles is  $5e8$ .
- (5) The friction coefficient between the spheres is 0.015, the damping ratio is 0.2, and the sphere density is set to 7800 kg/m<sup>3</sup>.
- (6) A measuring ball with a radius smaller than the inner diameter of the barrel is set at the outlet of the loading funnel, and a similar measuring ball is set up and down in the barrel to perform numerical simulation.
- (7) Set the random seed number to be large enough to ensure that the particle distribution of each verification experiment is consistent. The random seed number in this paper is 10001.
- (8) The physical time for each numerical simulation is set to 30s. The program automatically determines the time step based on the complexity of the calculated model.

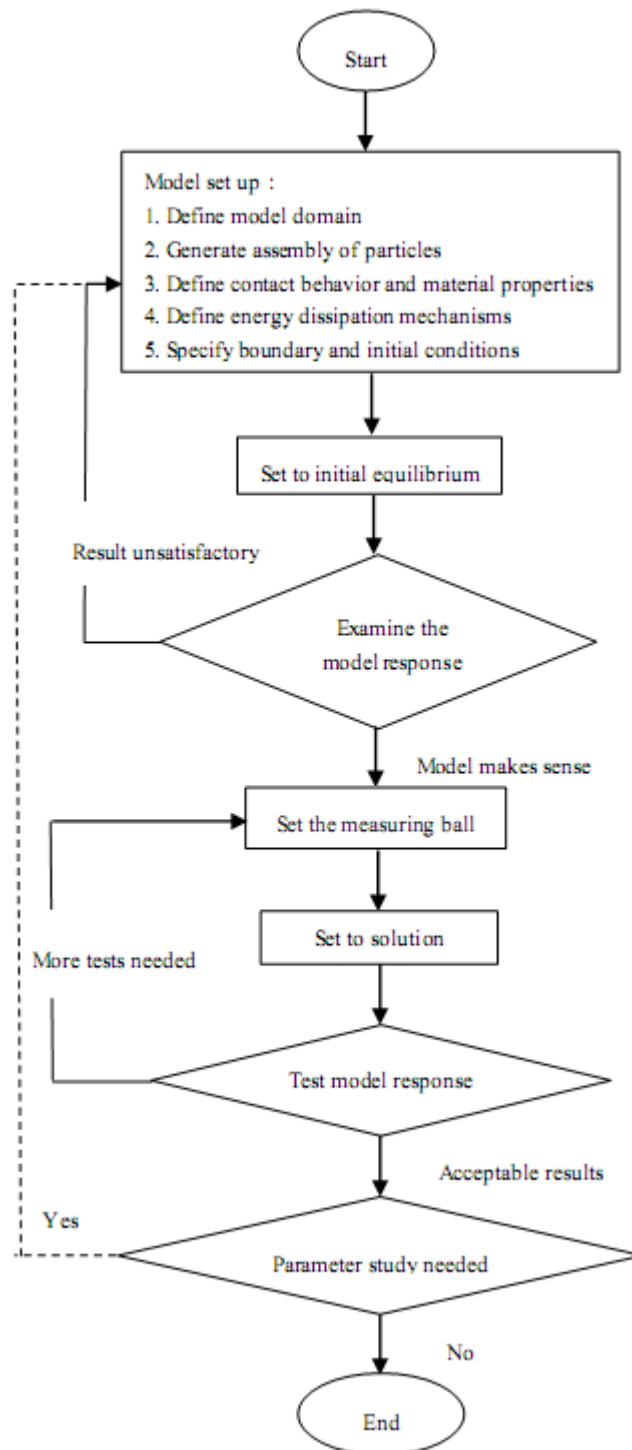


Fig. 1 Flowchart of operational phases

### 3.2 Simulation Process

#### 3.2.1 Modeling and Model Response

Program commands were written in FISH language to generate solution spheres, particles, walls,

and porosity measuring balls. Then, the barrier plane of the material outlet was removed through the program, so that the spheres naturally settled into the cylinder from the funnel bucket. Finally, the settlement was achieved. The granules are in a steady state, facilitating the reading of the final measurement from the porosity change curve. In the above simulation process, the initial parameters are set as described above, and the response to the model is observed and adjusted through the visualization window. A reasonable solution step length and time can be set according to the system operation status. The solution time used in this paper is 30s. The final settling particles are guaranteed to be in a steady state. At the same time as the preparation of the packing, a porosity measurement ball was set to measure the porosity change of the spherical particles at the outlet and inside the barrel during the falling of the ball.

### 3.2.2 Data detection

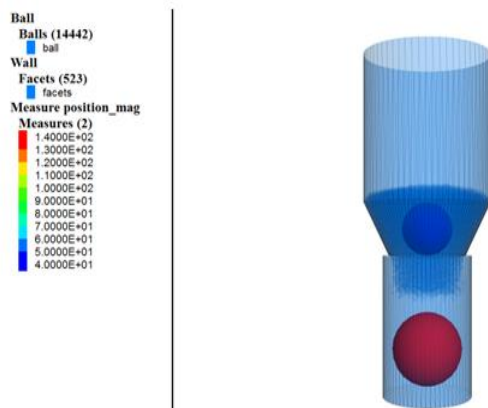


Fig. 2 Set porosity measurement ball

As shown in the Fig. 2, the vertical coordinate of the measuring ball set at the discharge port is  $40\mu\text{m}$ , the diameter of measuring ball is  $80\mu\text{m}$ , and the measuring ball with a larger radius is set inside the barrel to reduce the effect of local abnormal accumulation on the numerical value of the porosity. The coordinate is  $140\mu\text{m}$ , and the measuring ball diameter is  $110\mu\text{m}$ . The main porosity measuring ball is set inside the barrel, the barrel radius is  $70\mu\text{m}$ , and

the spherical particles have an average particle radius of  $30\mu\text{m}$ . The ratio of the wall radii to ball radii is about 23:1, which can effectively eliminate the influence of the boundary on the grain accumulation. By measuring the ball's reasonable settings, real-time monitoring of the porosity during particle accumulation can be achieved.

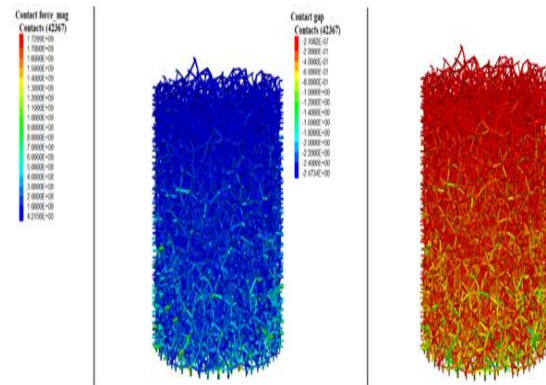


Fig. 3 Distribution of contact force Fig. 4 Contact Clearance Between Spheres

Fig. 3 represents the distribution of the contact force between particles, because the deposition of the lower particles not only inherit the role between adjacent particles, also from upper particles' gravity, in a container near the wall of contact force between particles and wall body to balance the internal contact force between particles, therefore, the size of the contact force distribution from top to bottom, from the inside out, in turn, the trend of increase, in the sphere - wall contact type compared with sphere - ball contact type of contact force is larger.

Fig.4 represents the contact clearance of every contact point. as can be seen from the diagram, each contact point are varying degrees of overlap, the particles rigidity and coordinates of the vertical have a significant influence to contact clearance. When the ball rigidity is certain, the contact clearance of the particle packing from the top to the bottom contact is gradually increasing, because the contact is overlapped, so it is negative.

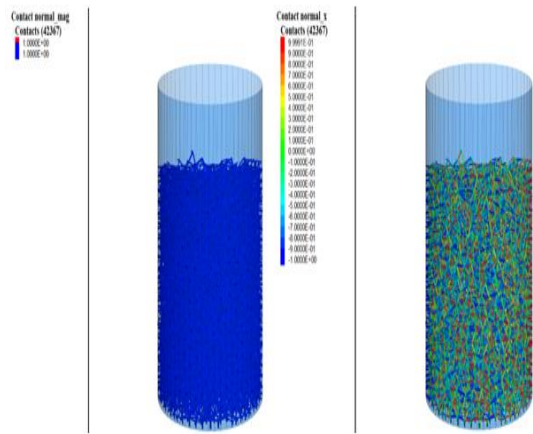


Fig. 5 Global Contact Normal ( X - axes )

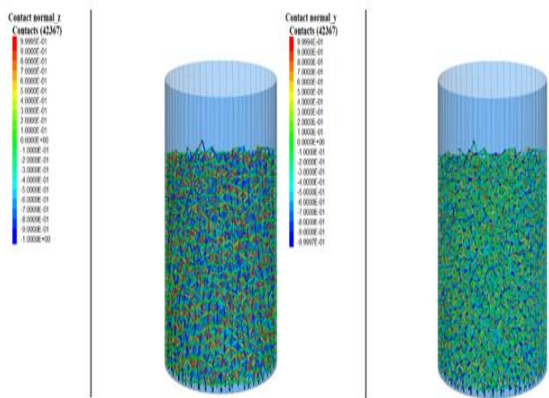


Fig. 7 Contact Normal ( Y - axes ) Fig. 8 Contact Normal ( Z - axes )

Fig. 5 shows that the global contact normal is 1. Fig. 6 -8 respectively represents the component value of contact normal in the direction of X, Y and Z axes. The simulation process about the particle size of normally distributed spherical particles with accumulation is simulated, by changing the size of normal distribution function, this paper is studied under the same average particle size, different variance of spherical particles to the influence of packing density. In only change the particle size of normal distribution function, the internal physical structure and mechanical properties keep the same

characteristics, By setting the measuring ball of porosity at a reasonable position inside the container, the real-time monitoring of the porosity inside the accumulation body can be realized. The quality of the spherical particle body distribution consistent with the particle size distribution, contact types are divided into sphere - wall and sphere - sphere, the contact force is not only related to the contact type, and the position of the sphere of the Z axes direction, a general from top to bottom, from the inside to out, in turn, the trend is increase, Because of the contact clearance should be negative, so the corresponding contact force is inversely proportional to the contact clearance. The contact type has great influence on the force and structure of the packing particles

Fig. 9 Porosity change curve of different measurement ball

As shown in Fig. 9, the red curve P6 is the porosity change curve of the outlet particle accumulation, and the yellow curve P7 is the porosity change curve of the particle accumulation in the cylinder. The total ball settlement process is available, as shown in the figure. When P6 is equal to 0.30, the pellets are in the state of preliminary packing. When P7 is equal to 0.28, the pellets are in the filling state.

Through the above modelling and model response, the accumulation porosity of particles with equal diameter of 30µm is finally stable at 0.28, while the theoretical value of the minimum porosity of equal diameter sphere is 0.2594, with a difference of only about 0.02, indicating the internal stacking structure of the barrel with medium diameter sphere. It is already quite close to the densest hexahedral type. It can be concluded that the experimental data obtained are in good agreement with the actual situation, indicating that the initial conditions set are more reasonable and can be used to do further research for the spherical particles with a normally distributed particle size.

### 3.3 Porosity Measurement of Spherical Particles with Normally Distributed Particle Size

In this paper, we study the packing density



of spherical particles, and set the mean particle size to 30 $\mu\text{m}$  to detect changes in particle porosity under different variance conditions. Modeling, model response, porosity testing process, time steps, and parameter settings are all consistent with the verification process described above, and only change the distribution of generated particles. Using the built-in program commands, particles with a mean value of 30 $\mu\text{m}$  and particle sizes that satisfy different variances were generated. Real-time porosity detection was performed on the sedimentation process of the particles.

### 3.3.1 Porosity change curve with mean particle size $\mu = 30\mu\text{m}$ and variable variance ( $\sigma$ )

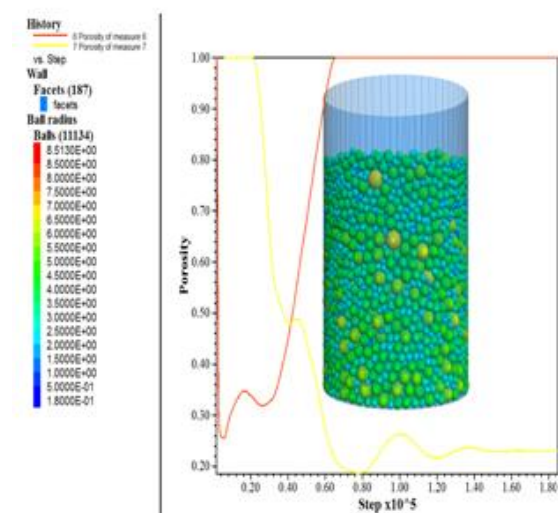


Fig. 10

Porositycurve( $\mu = 30\mu\text{m}$ ,  $\sigma = 12$ )

As shown in Fig. 10, the vertical axes represent the porosity value of the particle accumulation, the horizontal axes represent the time step of the particle calculation, because the internal operation amount difference, the required time step length is not the same, but the physical time is a fixed value of 30s. The curves of porosity changes under different variances are given in Appendix A.

The red curve P6 represents the change curve of the particle porosity at the feed port, and the yellow curve P7 represents the change curve of the particle porosity within the barrel. The color of

different particles in the cartridge represents the particle size of the particles. The distribution of the spheres passes through different particle sizes. The change of sphere color shows that the distribution of spherical particles with different variances can be intuitively obtained. As the variance increases, the differentiation of large and small particles becomes more obvious, and the particle size inside the particles gradually becomes larger.

### 3.3.2 Analysis of results

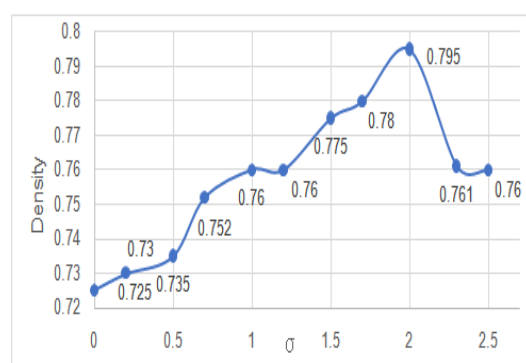


Fig. 11 DensityVariation with Increasing of  $\sigma$

The porosity change curve is as shown in the Fig 11, it can be found that as the variance  $\sigma$  increases, the density first increases and then decreases. At the same time, in terms of the porosity ratio, the distribution of the porosity of the spherical particles with a normally distributed particle size is lower than that of the identical sphere with the same particle size. Therefore, the packing density of multi-sized spheres is generally higher than mono-sized spheres. As the variance increases, for a spherical particle with a normally distributed particle size, the packing density first increases, then decreases, and finally there is a maximum packing density about 0.795.

## IV. CONCLUSION

The packing density of spherical particles with a normally distributed particle size is studied. The porosity variation curve of a spherical model with mean ( $\mu = 30\mu\text{m}$ ) and variance ( $\sigma$ ) is analyzed. Linear regression analysis is used to analyze the data

obtained. With the increase of  $\sigma$ , for the spherical particles with a normally distributed particle size, the change trend of the porosity is to decrease first and then increase, which is opposite to the change trend of the packing density. When  $\mu=30\mu\text{m}$  and  $\sigma=20$ , the spherical particles have the smallest porosity and the corresponding packing density reaches the maximum value of 0.795.

The mono-sized spheres ( $r = 30\mu\text{m}$ ) is used to verify the rationality of numerical simulation. By comparison with the porosity curve data obtained under different variance parameters, it is shown that as for spheres with a normal distribution, the packing density of particles is generally higher than the theoretical maximum value of 0.7406 for mono-sized spherical particles, and as the  $\sigma$  increases, indicating that the increase of  $\sigma$  promotes the increase of packing density, but when  $\sigma$  exceeds a certain value, there is a negative effect on the increase in packing density.

By comparison with Horsfield Compact Packing Theory, it is shown that the packing density of spherical particles with a normally-distributed particle size is generally between 0.7406 and 0.793. When  $\mu=30\mu\text{m}$  and  $\sigma=20$ , the packing density is 0.795, which is slightly higher than the theoretical packing density of the binary grading sphere model of 0.793, indicating that the packing density of spherical particles with normal distribution can achieve the theoretical packing density of binary spherical particles grading model.

## V. ACKNOWLEDGEMENT

This work was supported by the Fundamental Research Funds for the Central Universities (2017MS150).

## REFERENCES

- [1]. German R M. Particle packing characteristics [M], Metal Powder Industries Federation: Princeton, New Jersey, 1989.
- [2]. Bideau D, Hansen A. Disorder and granular media, random materials and process, Ed. H.E. Stanley and E. Guyon, Elsevier Science Publishers: North-Holland, Amsterdam, 1993.
- [3]. Bernal J D, Mason J. Coordination of randomly packed spheres [J], Nature, 1960, 188:910-911.
- [4]. Bernal J D. Optimization of multi-component hard sphere liquids with respect to dense packing [J], Proc. Roy. Inst., 1959, 37: 355.
- [5]. Scott G D. Packing of equal spheres [J], Nature, 1960, 188: 908-909.
- [6]. Scott G D, Charles worth A M, Mak M K. On random packing of spheres [J]. Chem. Phys. 1964, 40: 611-613.
- [7]. Finney J L. Random packing and the structure of simple liquids [J], Proc. Roy. Soc. Lond.A, 1970, 319: 479-493.
- [8]. cui gengyan, soil analysis, liu baojun's discussion on the preparation of metal powder [J]. Scientific and technological information, 2011(10)
- [9]. Aste T, Saadatfar M, Sakellariou A, et al .Investigating the geometrical structure of disordered sphere packings [J]. Physica A: Statistical Mechanics and its Applications, 2004, 33(9): 16-23.
- [10]. Echt O, Sattler K, Recknagel E. Magic numbers for sphere packings: experimental verification in free xenon clusters [J]. Physical Review Letters, 1981 , 47(16): 1121-1124.
- [11]. Anand A, Curtis J S, Wassgren C R, et al. Predicting discharge dynamics from a rectangular hopper using the discrete element method (DEM)[J]. Chemical Engineering Science, 2008, 63(24): 5821-5830.
- [12]. Cleary P W, Sawley M L. DEM modelling of industrial granular flows: 3D case studies and the effect of particle shape on hopper discharge [J]. Applied Mathematical Modelling, 2002, 26: 89-111.
- [13]. Hbhner D, Wirtz S, Scherer V. A numerical



- study on the influence of particle shape on hopper discharge within the polyhedral and multi-sphere discrete element method [J]. Powder Technology, 2012, 22(6): 16-28.
- [14]. An X, Li C. Experiments on densifying packing of equal spheres by two-dimensional vibration [J]. Particuology, 2013, 11(6): 689-694.
- [15]. An X Z, Li C X, Yang R Y, et al. Experimental study of the packing of mono-sized spheres subjected to one-dimensional vibration [JJ]. Powder Technology, 2009, 196(1):50-55.
- [16]. liu wensheng, peng fen, ma yunzhu, et al. Research progress in preparation of metal powder by aerosol method [J]. Material guide, 2009(3).
- [17]. lv hong, Chen zhenhua, Chen gang. Study on the atomization of solid-gas two-phase flow in liquid metal and alloy [J]. China powder technology, 2004(4).
- [18]. liu wensheng, ma yunzhu, huang boyun, et al. New technology and equipment for powder metallurgy [J]. Metallurgical engineering, 2007(5).
- [19]. liang rong, party xinan, zhao xiaojuan, et al. Design of ultrasonic atomizer nozzle [J]. Shanghai nonferrous metal, 2006(4).
- [20]. Yang lun zhuang, wu sun jianhui. Research status and prospect of the resource, use and extraction technology of chromium [J]. Iron alloy, 2010(6).